

²⁰L. Pauling, *The Nature of the Chemical Bond* (Cornell Univ. Press, Ithaca, N. Y., 1960), 3rd ed.

120 (1966).

²¹T. R. Anthony and D. Turnbull, *Appl. Phys. Lett.* **8**,

²²T. R. Anthony, J. W. Miller, and D. Turnbull, *Scr. Met.* **3**, 183 (1969).

Low-Lying Even-Parity Resonances in KI:Ag⁺

R. D. Kirby*

*Laboratory of Atomic and Solid State Physics,† Cornell University, Ithaca, New York 14850,
and Department of Physics and Materials Research Laboratory,‡ University of Illinois, Urbana, Illinois 61801*

(Received 14 September 1970)

Lattice resonances of E_g symmetry (16.35 cm^{-1}) and A_{1g} symmetry (25 cm^{-1}) have been found in KI:Ag⁺ using far-infrared spectroscopic techniques. The two even-parity modes are found to be anharmonically coupled to the T_{1u} -symmetry resonant mode at 17.3 cm^{-1} , giving rise to the combination bands observed at 30 and 44.4 cm^{-1} .

An optically active T_{1u} -symmetry resonance at 17.3 cm^{-1} in KI:Ag⁺ has been known for some time.¹ In general, there can also be impurity-activated quasilocalized resonances with even parity. Such modes are not optically active, and in the simplest approximation they involve motion only of the defect nearest neighbors. We wish to report here the identification of two even-parity resonances in KI:Ag⁺, one at 16.35 cm^{-1} with E_g symmetry, the other near 25 cm^{-1} with A_{1g} symmetry. These modes were detected by far-infrared absorption measurements with the KI:Ag⁺ sample in an external electric field. The field induces a strong mixing of the nearly degenerate E_g and T_{1u} modes, resulting in linear shifts of the mode frequencies. The A_{1g} mode also shifts linearly with applied field, but the field-induced mixing in this case is more complicated.

In addition, weak absorption lines at 30 and 44.4 cm^{-1} in zero field are attributed to the T_{1u} - E_g and T_{1u} - A_{1g} combination bands, respectively. The absorption strengths of these bands are a measure of the anharmonic coupling of the even modes to the odd mode.

The far-infrared absorption measurements were made using a lamellar interferometer² and a liquid-He³-cooled germanium bolometer.³ The instrumental resolution was typically 0.25 - 0.35 cm^{-1} . The techniques involved in making the electric-field-dependence measurements have been described elsewhere.⁴

The KI:Ag⁺ far-infrared absorption spectrum is shown in Fig. 1 for a sample temperature of 1.2°K . In addition to the strong resonant-mode transition at 17.3 cm^{-1} , there are five relatively weak lines. Also observed, but not shown in

Fig. 1, is a strong gap mode at 86.2 cm^{-1} . The two highest frequency lines, 55.8 and 63.5 cm^{-1} , can be correlated with host-crystal density-of-states peaks, after Dolling *et al.*⁵ The 30 - and 44.4-cm^{-1} lines are both asymmetric, with integrated absorption strengths relative to that of the resonant mode of 0.29 and 0.19 , respectively. It is these two lines which are important in the interpretation of the results to be presented here.

The results of a typical electric-field run are shown in Fig. 2. The dashed curve shows the KI:Ag⁺ T_{1u} -symmetry resonant-mode absorption line in zero field. The solid curve shows the observed absorption spectrum with an external electric field (E_{dc}) of 130 kV/cm applied in the $[100]$ crystallographic direction and the E vector of the incident radiation (E_{ir}) polarized parallel to E_{dc} . With the field applied, there are two absorption lines in the 17-cm^{-1} region. The higher frequency of these two peaks is due to the field-shifted component of the T_{1u} mode. Clearly, the absorption strength of this line decreases with increasing field. The lower-frequency peak appears only when a field is applied. It increases

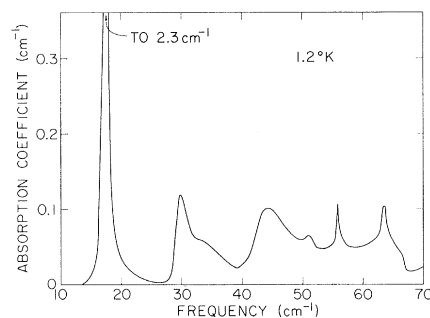


FIG. 1. KI:Ag⁺ far-infrared absorption spectrum.

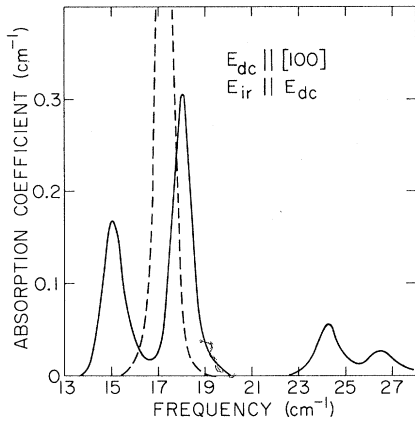


FIG. 2. Typical electric-field-induced frequency shift. The dashed curve is for 0 kV/cm, the solid curve for 130 kV/cm.

in strength with increasing field and shifts to lower frequencies. These effects are characteristic of two modes of opposite parity being mixed by the (odd-parity) electric field.

In Fig. 2, the absorption line at 26.5 cm^{-1} is due to a field-shifted component of the 30-cm^{-1} line of Fig. 1. It decreases in strength with increasing field and shifts down in frequency. The 24.2-cm^{-1} line appears only when a field is applied. It grows in strength with increasing field and also shifts to lower frequencies. The field-induced mixing in this case is more complicated since both lines shift down in frequency. This is most likely caused by the presence of the E_g - and T_{1u} -mode second harmonics in the 30 - to 35-cm^{-1} region.

[100] field measurements have been made for $E_{ir} \parallel E_{dc}$ and $E_{ir} \perp E_{dc}$. For a [110] electric field, there are three distinct polarization directions, corresponding to $E_{ir} \parallel E_{dc}$, $E_{ir} \parallel [1\bar{1}0] \perp E_{dc}$, and $E_{ir} \parallel [001] \perp E_{dc}$. Field-dependence measurements have been made for all three polarizations. For a [100] field, both the 16 - and 25-cm^{-1} lines were observed only for $E_{ir} \parallel E_{dc}$. The 25-cm^{-1}

line was not observed at all with a [110] field applied, while the 16-cm^{-1} line was observed for $E_{ir} \parallel E_{dc}$ and $E_{ir} \parallel [1\bar{1}0]$. We now use these results to determine the symmetries of the two modes. With a [100] external field, the defect site symmetry is reduced from O_h to C_{4v} , so that an E_g mode in O_h splits into two levels, transforming as the A_1 and B_1 irreducible representations of C_{4v} . Of these, only the A_1 is optically active, and then only for $E_{ir} \parallel E_{dc}$. For a [110] field, the site symmetry becomes C_{2v} and an E_g mode splits into levels transforming as the A_1 and B_1 irreducible representations of C_{2v} . Both of these levels are optically active, the A_1 for $E_{ir} \parallel E_{dc}$, and the B_1 for $E_{ir} \parallel [1\bar{1}0] \perp E_{dc}$. This analysis agrees with the experimental results for the 16-cm^{-1} line and thus confirms that the mode in zero field has E_g symmetry.

An A_{1g} mode should be observed with $E_{ir} \parallel E_{dc}$ for both [100] and [110] fields, but not for $E_{ir} \perp E_{dc}$. The Ag^+ concentrations in the samples used for the $E_{ir} \parallel E_{dc} \parallel [110]$ measurements were apparently too low for either the 25-cm^{-1} line or shifts of the 30-cm^{-1} line to be observed. It is more significant that the 25-cm^{-1} line was *not* observed when $E_{dc} \parallel [110]$ and $E_{ir} \parallel [1\bar{1}0]$, even though shifts of the 30-cm^{-1} line were observed. In view of this, we conclude that the even-parity mode near 25 cm^{-1} does have A_{1g} symmetry.

We now show that many of the experimental results can be explained by introducing an anharmonic interaction between the T_{1u} mode and the two even modes. We first assume that the three modes can be represented as independent harmonic oscillators. Then the lowest-order anharmonic interaction between the odd mode and the two even modes consistent with the octahedral symmetry at the impurity site must be of the form $Q_{\text{odd}}^2 Q_{\text{even}}$. More specifically, for our particular choice of normal coordinates,⁶ the most general form of the interaction is

$$\mathcal{H}_A = A(2Q_{T_1}^2 Q_{E_1} - Q_{T_2}^2 Q_{E_1} + \sqrt{3} Q_{T_2}^2 Q_{E_2} - Q_{T_3}^2 Q_{E_1} - \sqrt{3} Q_{T_3}^2 Q_{E_2}) + B(Q_{T_1}^2 + Q_{T_2}^2 + Q_{T_3}^2) Q_A. \quad (1)$$

Here, the Q 's are the mode normal coordinates in an obvious notation. We treat \mathcal{H}_A as a perturbation, finding the second-order perturbed energies and the first-order perturbed eigenvectors.

One obvious manifestation of this type of anharmonic coupling is that the combination bands, corresponding to the simultaneous excitation of one even-mode quantum and one odd-mode quantum, are made optically active. The combination-band frequencies will not be at exactly the

sum of the even- and odd-mode frequencies because of the coupling. The strengths of the combination bands are a measure of the coupling coefficients A and B . Assuming that the 30 - and 44.4-cm^{-1} lines are the E_g - T_{1u} and A_{1g} - T_{1u} combination bands, respectively, we use the measured absorption strengths to calculate $A = 5.7 \times 10^{11}$ erg/cm³ and $B = 1.8 \times 10^{12}$ erg/cm³. In this calculation, it is assumed that the mode harmon-

Table I. Calculated electric field shifts.

E_{dc}	Polarization	E_{ir}	Calculated shifts ^a
[100]		[100]	$\pm(\Delta^2 + R^2 E_i^2)^{1/2}$
[100]		[001]	0
[110]		[110]	$\pm(\Delta^2 + \frac{1}{4} R^2 E_i^2)^{1/2}$
[110]		[110]	$\pm(\Delta^2 + \frac{3}{4} R^2 E_i^2)^{1/2}$
[110]		[001]	0

$$^a R = \frac{2e_0^* \hbar A}{\Omega(E_g)M(T_{1u})[2\Omega(T_{1u}) - \Omega(E_g)][M(T_{1u})\Omega(T_{1u})M(E_g)\Omega(E_g)]^{1/2}}$$

ic frequencies may be approximated by the observed transition frequencies.

The cubic anharmonicity will also allow an electric field to mix the even- and odd-parity modes. The coupling between the A_{1g} and T_{1u} modes is expected to be less important because of their greater energy separation and will not be included here. The application of an external electric field in the [100] direction then introduces the perturbation

$$\mathcal{H}_E = -e_0^* E_i Q_{T_{1u}}, \tag{2}$$

where e_0^* is the effective charge associated with the odd-parity mode, and E_i is the local electric field at the impurity site. Since the E_g and T_{1u} modes are nearly degenerate, we let 2Δ be their zero-field separation and do first-order degenerate perturbation theory with \mathcal{H}_E . This leads to a mixing of the (anharmonic) E_g and T_{1u} modes, resulting in the field-induced shifts

$$W(E_i) = \pm(\Delta^2 + R^2 E_i^2)^{1/2}, \tag{3}$$

where R is as given in Table I. The plus and minus signs in Eq. (3) are to be associated with the T_{1u} and E_g modes, respectively. The results of this calculation for the various field and polarization directions are summarized in Table I.

The field-dependent shifts of the E_g and T_{1u} modes are summarized in Fig. 3, which shows the absorption frequencies as a function of the external field. The frequency shifts in all cases are found to be linear with field in the high-field limit. Because of the nonzero splitting in zero field, the mode frequencies are expected to show a quadratic dependence on E_{dc} in the low-field region. The curves of frequency versus field for the E_g mode could not be extended into the low-field region because of its vanishing absorption strength. For these reasons, the zero-field frequency of the E_g mode is known only to an accuracy of $16.35 \pm 0.1 \text{ cm}^{-1}$.

The solid curves in Fig. 3 show the calculated shifts of Table I. The value of R (and hence of A) has been chosen to fit the [100] field dependence of the E_g mode. The agreement for the other E_g -component shifts is quite satisfactory, and so offers conclusive evidence that third-order anharmonicity is the dominant mixing mechanism involved. Setting $e_0^* = e$, $M(T_{1u}) = M(\text{Ag}^+) = 108 \text{ amu}$, $M(E_g) = M(I^-) = 127 \text{ amu}$, and making the Lorentz local-field correction, we calculate $A = 3.7 \times 10^{11} \text{ erg/cm}^3$. This is considered reasonable agreement with the earlier estimate of A in view of the experimental uncertainties involved and the approximations which have been made.

The experimental shifts of the T_{1u} -mode components are all smaller than the calculated values. This indicates that mixing of the A_{1g} and T_{1u} modes should also be considered. There

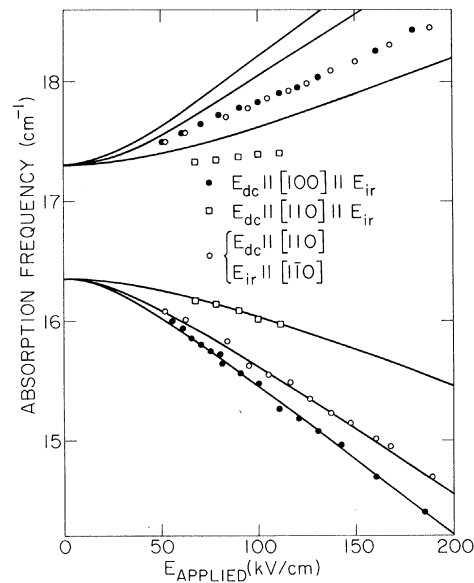


FIG. 3. Summary of the electric-field-dependence results. The solid curves were obtained by fitting to the E_g -mode [100] field shifts (closed circles).

must, however, be other contributing factors, such as coupling to the host crystal phonons, since the E_g - and T_{1u} -mode components do not shift equal amounts when $E_{dc} \parallel [110]$ and $E_{ir} \parallel [1\bar{1}0]$. In this particular field configuration, the A_{1g} - T_{1u} mixing cannot cause any shifts.

While not yet fully understood, the results presented here reveal several important properties of the KI:Ag⁺ lattice-defect system. Perhaps the most striking features are the very low frequencies of the even-parity resonances. Benedek and Nardelli⁷ have calculated the A_{1g} and E_g Green's functions for impurities in KI using a model in which only the nearest-neighbor force constants were allowed to change. Using their Green's functions, it is easy to show that the effective force constant reaches zero long before the even-parity resonances reach such low frequencies. This makes obvious the need for more realistic defect models.

The electric-field-dependence measurements and the observation of what appear to be the even-odd combination bands offer the first conclusive evidence of a strong dynamical coupling between even- and odd-parity resonances. This type of coupling may also play a major role in the temperature-dependent properties of resonant modes.⁸ It should be noted here that this E_g mode is quite likely the cause of the thermal conductivity resonance observed by Bauman and Pohl⁹ in KI:Ag⁺. If so, their estimated frequency of $12 \text{ cm}^{-1} \pm 20\%$ is somewhat low. Since the even-parity mode frequencies are important parameters in dynamical lattice-defect models, it appears that such

modes will assume an increasing importance in the further study of lattice resonant mode systems.

The author would like to thank Professor A. J. Sievers and Professor M. V. Klein for helpful discussions and comments on the manuscript.

*Present address: Department of Physics, University of Illinois, Urbana, Ill. 61801.

†Research supported by the U. S. Atomic Energy Commission under Contract No. AT(30-1)-2391, Technical Report No. NYO-2391-121. Additional support was received from the Advanced Research Projects Agency through the Materials Science Center at Cornell University.

‡Work supported in part by the Advanced Research Projects Agency under Contract No. HC 15-67-C-0221.

¹R. D. Kirby, I. G. Nolt, R. W. Alexander, Jr., and A. J. Sievers, *Phys. Rev.* **168**, 1057 (1968).

²I. G. Nolt, R. D. Kirby, C. D. Lytle, and A. J. Sievers, *Appl. Opt.* **8**, 309 (1969).

³H. D. Drew and A. J. Sievers, *Appl. Opt.* **8**, 2067 (1969).

⁴B. P. Clayman and A. J. Sievers, *Phys. Rev. Lett.* **21**, 1453 (1968); B. P. Clayman, R. D. Kirby, and A. J. Sievers, to be published.

⁵G. Dolling, R. A. Cowley, C. Schittenhelm, and I. M. Thorson, *Phys. Rev.* **147**, 577 (1966).

⁶M. V. Klein, in *Physics of Color Centers*, edited by W. B. Fowler (Academic, New York, 1968), Chap. 7.

⁷G. Benedek and G. F. Nardelli, *J. Chem. Phys.* **48**, 5242 (1968).

⁸R. W. Alexander, Jr., A. E. Hughes, and A. J. Sievers, *Phys. Rev. B* **1**, 1563 (1970).

⁹F. C. Bauman and R. O. Pohl, *Phys. Rev.* **140**, A1030 (1965).